

## The Effect of Tool Geometry on the Microstructure and Mechanical Properties of Friction Stir Processed MIG-Welded Aa5083-H111

H. H. El-Fahhar <sup>1</sup>, H. Abd El-Hafez <sup>2</sup>, M. M. Z. Ahmed <sup>3</sup>,  
, Essam Ahmed<sup>3</sup>, A. El-Nikhaily <sup>1</sup>

<sup>1</sup>Mechanical Dep., Faculty of Industrial Education, Suez University, Egypt.

<sup>2</sup>Prod. Eng. & Mech. Design Dep., Faculty of Engineering, Port Said University, Egypt.

<sup>3</sup>Metallurgical and Materials Eng. Dep., Faculty of Petroleum & Mining Engineering, Suez University, Egypt.

<sup>4</sup> Mechanical Eng. Dep., Faculty of Engineering, the British University in Egypt, El-Sherouk City 11837 Cairo, Egypt.

Corresponding Author: H. H. El-Fahhar

---

**Abstract :** In this research, three different tool geometries (pinless, cylindrical and square pin) were developed to study the effect of friction stir processing (FSP) tool geometry on microstructure and mechanical properties of metal inert gas (MIG) welds 5083-H111 aluminum alloy. MIG welds and FSP specimens were evaluated using microstructure examination, tensile, and hardness tests. The microstructure investigation of FSP specimens reveals a very fine grain size in the processed zone, and reduction of welds defects compared to MIG welds. FSP of weld surface without reinforcement improved the tensile strength when compared with MIG welds, when pinless tool is used. In addition, the processed zone record higher hardness values than the base metal as well as the MIG welds.

**Keywords** –Friction stir processing, MIG welding, 5083 aluminum alloy, microstructure, mechanical properties

---

Date of Submission: 09-07-2018

Date of acceptance: 23-07-2018

---

### I. Introduction

AA5083 alloy is considered one of the most widely used alloys in the aerospace, shipbuilding, and automobile applications due to its lightweight and good corrosion resistance, higher strength combined with good formability, machinability and weldability [1, 2]. The MIG welding process is widely used in welding of AA5083, however, this process sometimes resulted in some defects such as solidification porosity, hot cracking, lack of wetting, which are very common in fusion welding processes [3, 4].

Friction stir processing (FSP) is a new solid state technique used to improve the microstructural properties and to eliminate the casting and welding defects such as porosity, thereby improving strength and ductility [5, 6].

Mishra et al. [7] investigated the effect of FSP parameters on the grain size of 2507 super duplex stainless steel. They reported that the better grain refinement could be achieved with increasing travel speed and higher heat input. Vaira et al. [8] studied the influence of FSP parameters on the wear resistance of aluminium alloy AA5083. The results revealed that the FSP refined the microstructure of the material and increased the hardness, and therefore increased the wear resistance of the material.

FSP is also, used to repair cracks and improve properties of fusion welded materials [9-13]. Gunter et al. [9] investigated the influence of FSP as a technique of repairing cracks in 12 mm thick 304L stainless steel plate. They reported that the FSP successfully in crack repair, and grain refinement, thereby the hardness increased when compared to base metal.

Jesus et al. [10] used FSP to improve the fatigue strength of MIG welding AA 5083. They reported that the FSP increases the hardness, but reduces the elongation on fracture of tensile specimens. Moreover, the fatigue strength was improved because of the grain refinement. Also, Jesus et al. [11] studied the effect of tool geometry on FSP, and fatigue strength of MIG T-welds on Al alloys. They concluded that the FSP tools with concave and rounded edge shoulder; cylindrical threaded pin removes defects in the MIG weld toe and improved of fatigue strength of MIG welds.

Borrego et al. [12] investigated the fatigue life improvement by FSP for 5083 aluminium alloy MIG butt welds. They proved that the fatigue resistance were improved due to microstructure grain refinement and the removal of welding defects. Fuller and Mahoney [13] examined the effect of FSP on the microstructural and

mechanical properties of MIG welds 5083-H321/5356. They reported that the FSP improved tensile strength, yield strength, elongation, and fatigue strength.

The aim of this research is to investigate the effect of tool geometry on microstructure and mechanical properties of friction stir processed MIG welded AA5083-H111.

## II. Experimental Procedure

### 2.1 Materials

The material used in this research was aluminum magnesium alloy AA5083-H111 of 6 mm thick wrought plate. AA5083 is a non-heat treatable aluminum alloy that can be strain hardened to a moderately high strength and very high toughness [14]. The AA5083 was chemical analyzed to obtain its chemical composition. The material was tested using tensile, and hardness tests to evaluate its mechanical composition and mechanical properties of AA5083-H111. Tables 1 and 2 summarize the chemical composition and mechanical properties of AA5083-H111.

**Table 1.** Chemical composition of AA 5083-H111 (wt. %).

Materials	Chemical Composition [%]								
Alloy	Si	Fe	Cu	Mn	Mg	Cr	Zn	Ti	Al
<b>5083-H111</b>	0.40	0.40	0.10	0.40-1.00	4.00-4.90	0.05-0.25	0.25	0.15	Rem.

**Table 2.** Mechanical proprieties of AA 5083-H111.

Materials	Mechanical Properties			
Base Metal	Ultimatetensile strength, UTS (MPa)	Yield strength YS (MPa)	Elongation %	Hardness (HV)
<b>5083-H111</b>	285	125	20	75

### 2.2 MIG Welding Procedure

MIG welding process were performed at the Oceandro Company, Suez- Egypt. The base material plates edges were prepared as shown in Fig. 1(a), according to structural welding code AWS D1.2/D1.2M [15]. The plates were welded in two passes as schematically illustrated in Fig. 1(b). Before performing the second weld pass, the root of the first weld was cleaned using stainless steel brush to obtain good fusion between the weld layers. The filler metal SFA/AWS A5.10: ER 5356, 1.2 mm in diameter, and pure argon was used in MIG welding. The MIG welding parameters that used are given in Table 3. Fig. 2 shows the macrograph of the butt joint after welded.

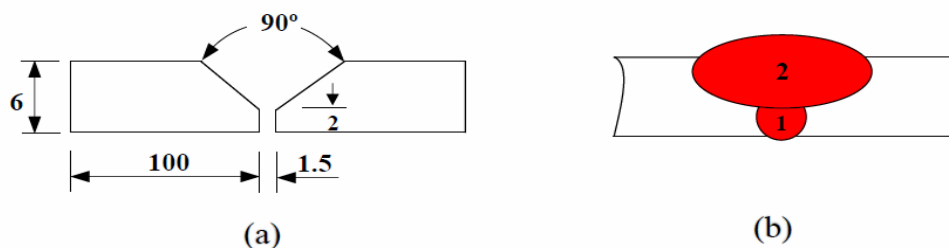


**Fig. 1** MIG welding preparation: (a) Joint preparation (dimensions in mm) and (b) Schematic representation of the pass sequence.

**Table 3.** MIG welding parameters.

Pass No.	Process	Size of filler (mm)	Current (A)	Voltage (V)	Travel speed (mm/min)	Torch distance (mm)
1st and 2nd	MIG	1.2	137	21.8	400 - 420	15

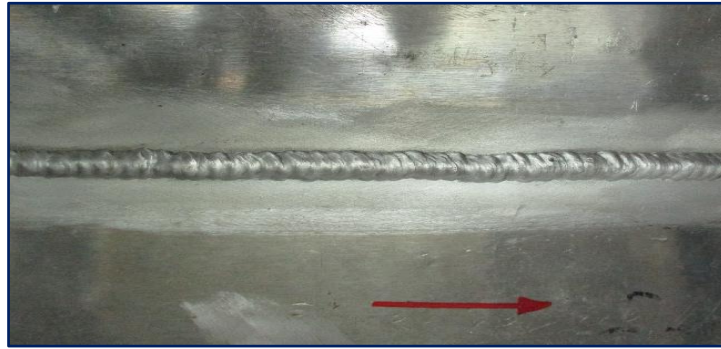
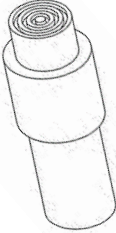
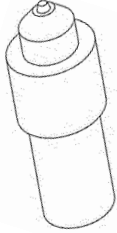
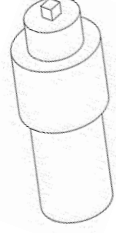


Fig. 2 Macrograph of MIG welded AA5083-H111 (Butt joint, Vertical, 3G).

### 2.3 Friction Stir Processing of MIG Welds

The friction stir processing of MIG welded AA5083 was performed using Egyptian Friction Stir Welding Machine 1 (EG-FSW-M1), which allowed control of the tool speed rotation and travel, and the vertical force on the tool. The tool material used was H13 (W302), and this tool was heat-treated to reach 52 HRC after machining. Three different tool geometries were developed and tested to study the effect of FSP on the microstructure and mechanical properties of MIG welded AA5083 aluminum alloy. Table 4 illustrates the geometries of the tool used for processing MIG welded AA5083.

Table 4. Tool geometries used in the present research: Pinless tool (tool 01), cylindrical pin (tool 02), and square pin (tool 03).

Tool Parameters	FSP Tools		
	Tool 01	Tool 02	Tool 03
Tool geometry	 Pinless	 Cylindrical pin	 Square pin
Pin length (mm)	Pinless	3	5.7
Shoulder diameter (mm)	28.6	10	25
Pin diameter (mm)	Pinless	6 tapering to 4	6×6

The pinless tool (tool 01) consists of three concentric circular equally spaced slots of 2 mm in depth on the shoulder surface; this tool was used for FSP of MIG welded surface without reinforcement (the root and crown surfaces of the MIG welds were milled) as shown in Fig. 3(a). While the tool 02 was used for FSP of MIG weld toes with reinforcement as shown Fig. 3(b). The tool 03 with a square pin is used for FSP of MIG welded plate without reinforcement as shown in Fig. 3(c).

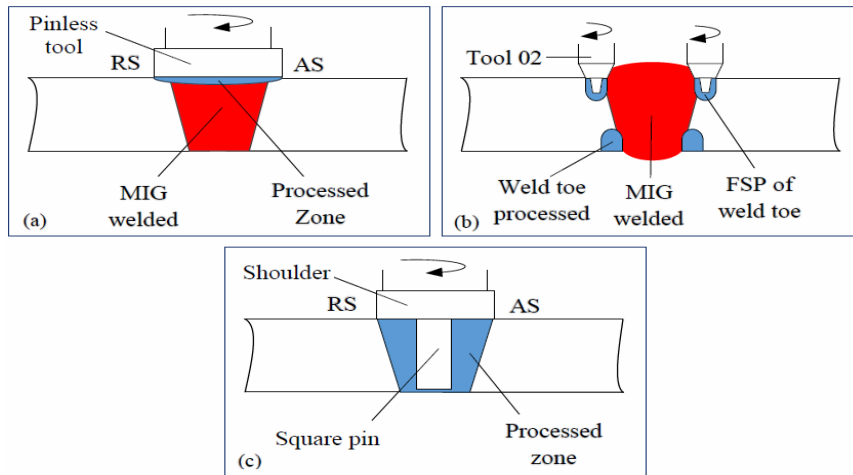


**Fig. 3** Schematic representation of FSP: (a) FSP of weld surface with tool 01, (b) FSP of weld toe with tool 02, and (c) FSP of MIG welded with tool 03.

The FSP parameters are presented in Table 5. These parameters were chosen based on previous studies and tests [13, 16, and 17]. The root and crown surfaces were processed by FSP in a single pass by pinless tool centered on the weld line as shown in Fig. 4. The weld toes were processed by FSP, one pass for each weld toe by cylindrical pin tool moving along each of the weld toes as shown in Fig. 5. MIG welded (without reinforcement) was processed by FSP, in a single pass by square pin tool (tool 03) as shown in Fig. 6.

**Table 5.** Friction stir processing parameters for all FSPs

Tool	Rotational speed (rpm)	Traverse speed (mm/min)	Average axial force (N/m)	Tilt angle $\alpha$ ( $^{\circ}$ )
Pinless tool				
Cylindrical pin	400	100	70	3
Square pin				

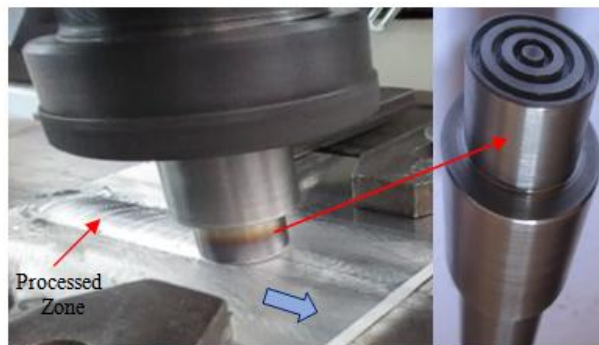


**Fig. 4** Photographs of FSP 01: Weld surface processed using tool 01 (Pinless).

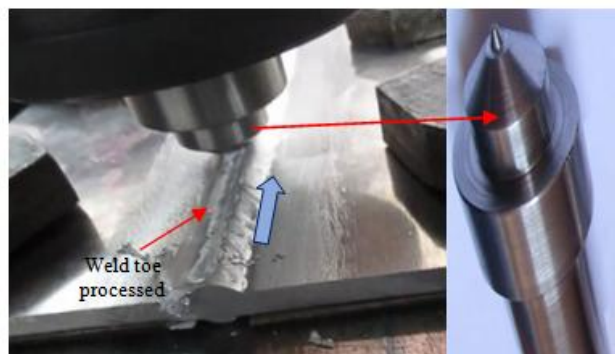


**Fig. 5** Photographs of FSP 02: Weld toe processing using tool 02.

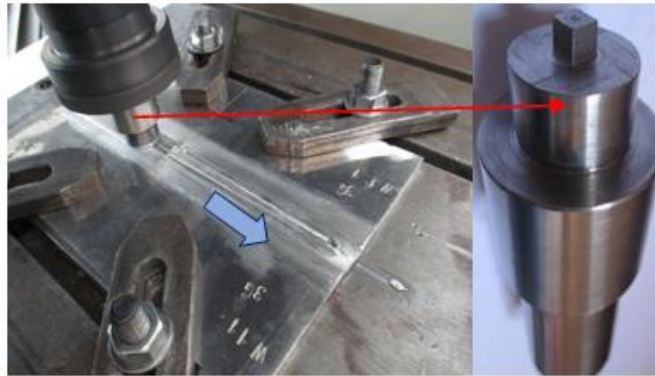


Fig. 6 Photographs of FSP 03: MIG welded processed using tool 03 (Square pin).

## 2.4 Characterization

Microstructural valuation of MIG welds, and FSPed specimens were investigated using optical microscope and scanning electron microscope (SEM). The traverse specimens were cut from the welds (40×15×6 mm) then ground and polished; according to standard metallographic practice ASTM E3-11 [18], Keller's reagent (3ml HCl, 5ml HNO<sub>3</sub>, 2ml HF, and 190 ml Distilled H<sub>2</sub>O) is used as etching agent to reveal the different microstructural features [19].

The microhardness test was carried out according to the ASTM E 348-11e1 standard [20] using Vickers microhardness tester. The test is performed using 200g as load at 15 sec. The hardness profile was through the cross section at 1.5 mm from the weld surface, and on processed surface for every 1 mm starting from weld center.

Tensile test was performed using the universal testing machine at room temperature with a constant across head speed of 0.1 mm/sec. The specimens were cut and machined to the required dimensions perpendicular the weld line according to standard ASTM E8M-04 [21] shown in Fig. 7. In each condition, three specimens were tested, and the average of the three results is presented in Table 6.

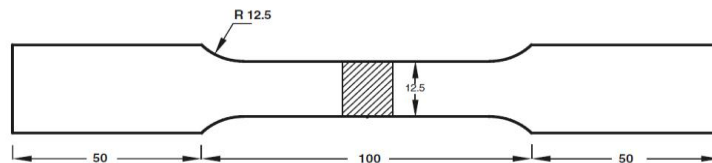


Fig. 7 Schematic of tensile specimen (dimensions in mm), [21].

## III. Results And Discussion

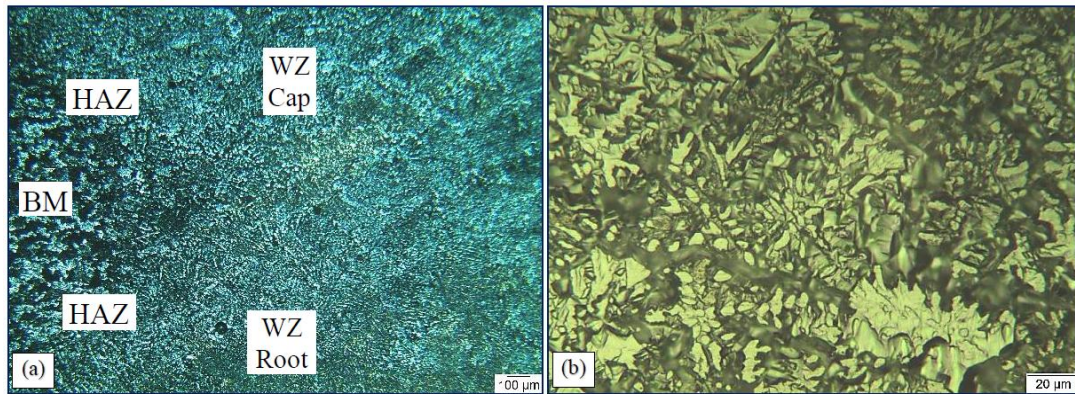
### 3.1 Microstructure of MIG Welds

Fig. 8 shows the optical macrograph for the cross section of the MIG welded AA5083-H111. The different regions are indicated on MIG weld macrograph namely, base metal (BM) (5083-H111 Al), fusion line (FL), weld zone (WZ), heat affected zone (HAZ) surrounding the weld zone, and weld toe (WT). Optical microstructure of MIG welded is shown in Fig. 9. The microstructure of base metal shows the elongated grains in the rolling direction; these grains were partially destroyed in the heat affected zone as shown in Fig. 9 (a). Moreover, the microstructure of weld zone contains of dendritic structure, which can be seen in Fig. 9 (b).



Fig. 8 Cross section analysis of MIG welded AA5083-H111: base metal (BM), fusion line (FL), weld zone (WZ), heat affected zone (HAZ), and weld toe (WT).





**Fig. 9** Microstructure of MIG welded AA5083-H111: (a) microstructural regions (BM, HAZ, and WZ), and (b) weld zone.

Scanning electron micrographs (SEM) of MIG welded are illustrated in Fig. 10. Whereas Fig. 10(a) shows solidification porosity in weld zone, lack of wetting defect is noticed in toe of weld root as Fig. 10(b). Furthermore, the SEM micrograph in Fig. 10(c) showed that the weld metal contains large dark and bright particles. According to Fuller and Mahoney [13], The dark and bright phases indicates  $Mg_2Si$  and  $Al_6(Mn, Fe)$  compounds, respectively.

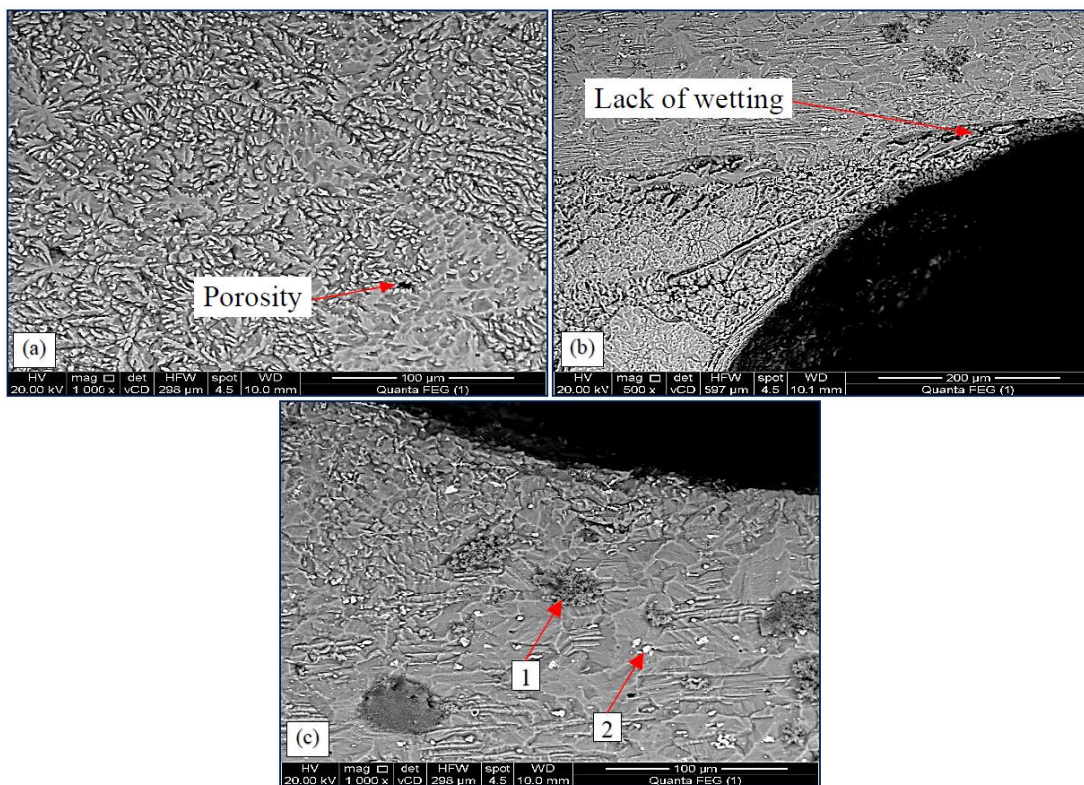


**Fig. 10** SEM micrographs analysis of MIG welded AA5083-H111: (a) weld zone, (b) weld toe at crown, and (c) weld zone (1)  $Mg_2Si$  and (2)  $Al_6(Mn, Fe)$  particles.

### 3.2 Microstructure of FSPed-MIG welds

From microstructure of MIG welded, it was observed that, the weld nugget contains dendritic structure and solidification porosity defects. Also, the weld toe contains defects called lack of wetting. These defects in MIG welds have motivated to using friction stir processing (FSP) to modify and improve the microstructure and mechanical properties of MIG welds. The root and crown surfaces of MIG welded were processed, without reinforcement, in a single pass by pinless tool. Fig. 11(a) illustrates optical microstructure of weld zone, and stirred zone under shoulder of tool 01. Fig. 11(b) shows the microstructure of stirred zone at weld top surface which contains the dark and bright grains,  $Mg_2Si$  and  $Al_6(Mn, Fe)$  compounds, respectively. The



microstructures of FSP regions contained smaller constituent particles and finer precipitates than those found in MIG welds [12, 13].

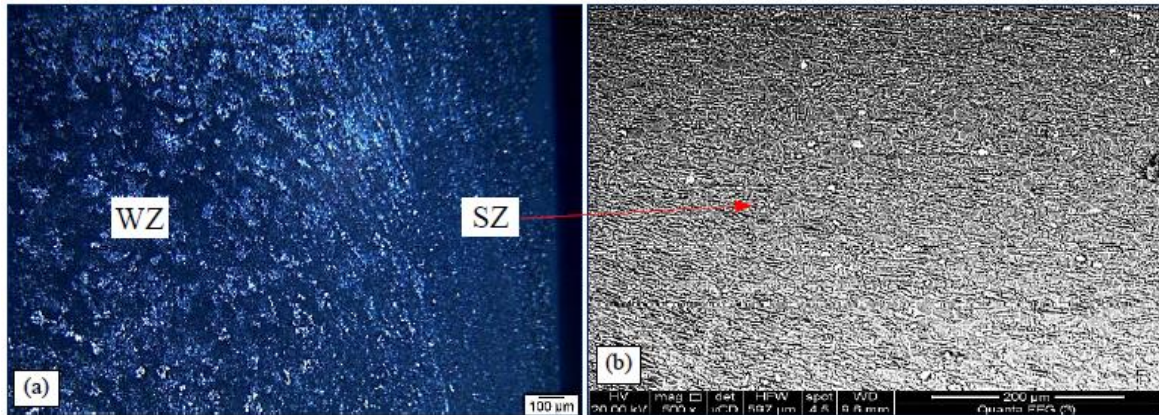


Fig. 11 Microstructure of FSP for MIG welded surface without reinforcement (pinless tool): (a) optical image, and (b) SEM of stirred zone.

Friction stir processing (FSP) was applied on all weld toes with reinforcement, one pass for each weld toe by cylindrical pin tool. Fig. 12(a) shows the microstructure observed after processing of weld toe, where, the wormhole defect was observed at 3.5 mm depth of weld toe surface, fig. 12(b). This defect maybe formed due to the FSP parameters (tool geometry, rotation and travel speed). Fig. 12(c) shows the microstructure of stirred zone at weld toe which contains the dark (1) and bright (2) grains,  $Mg_2Si$  and  $Al_6(Mn, Fe)$ .

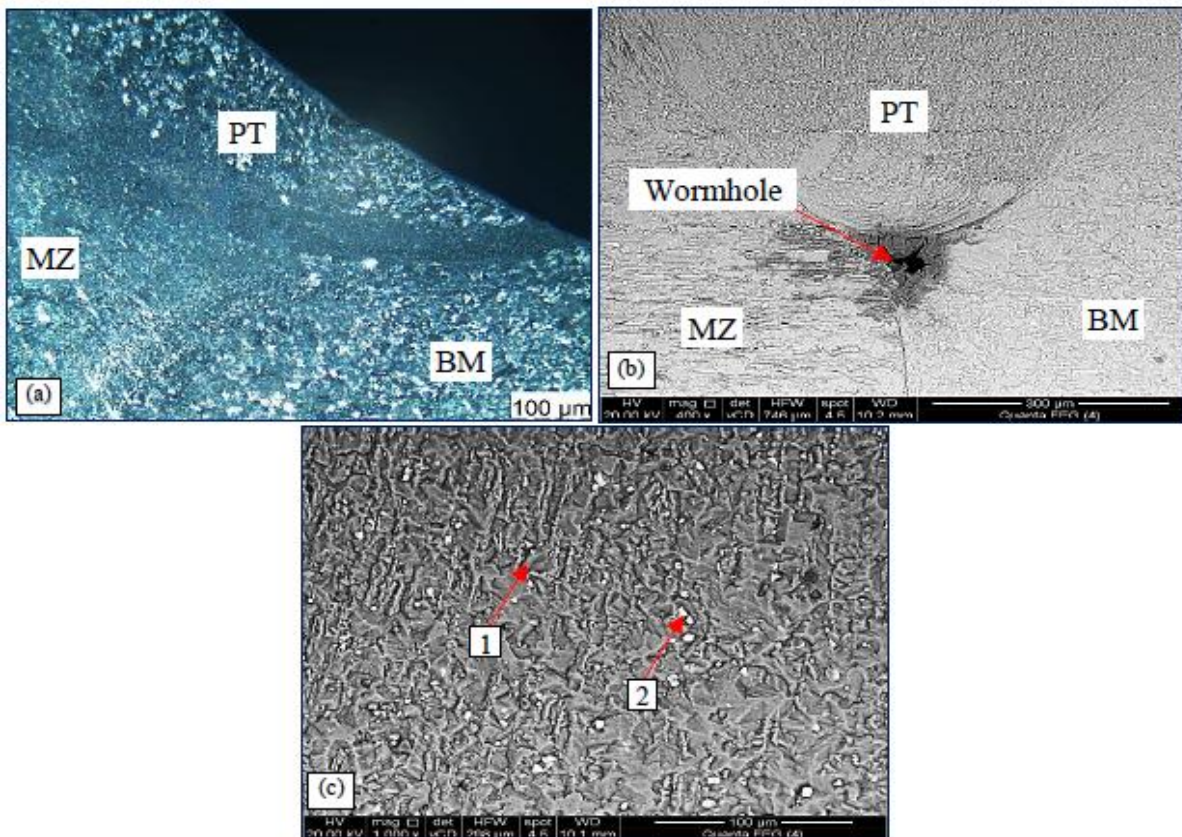
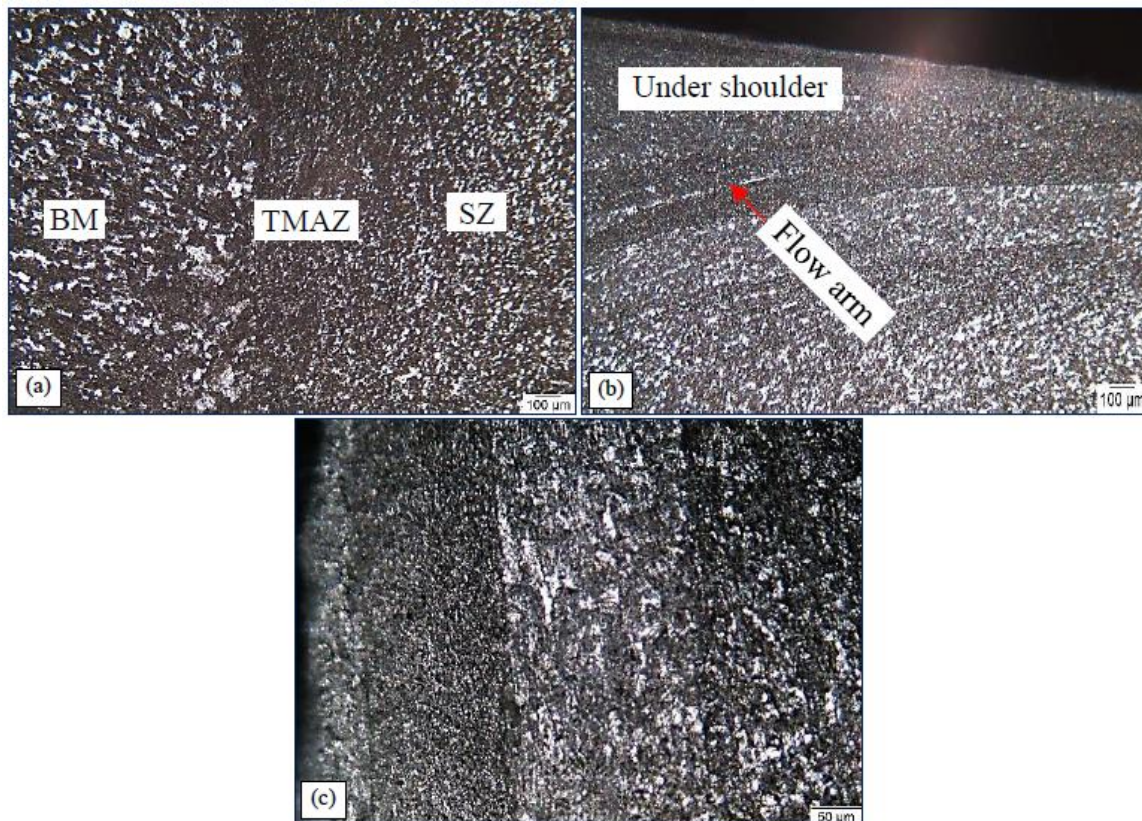


Fig. 12 Microstructure of FSP on weld toes with reinforcement (cylindrical pin tool): (a) optical microstructure regions, (b) SEM of processed toe (PT), and (c) processed zone (1)  $Mg_2Si$  and (2)  $Al_6(Mn, Fe)$  grains.



The effect of FSP using square pin tool on the joint microstructure is shown in Fig. 13, where the interface between the stirred zone (SZ) and base metal is noticed in Fig. 13(a). The microstructure of weld zone, where the flow arm is formed on the upper surface of the stirred zone as shown in Fig. 13 (b), where the FSP effect is clear in material movement from the retreating side to the advancing side. A very fine structure is formed, and there is a homogeneous distribution of severely fragmented precipitates. This fine structure is formed due to severe plastic deformation, caused by the tool shoulder rotation in the upper part of the stir zone as shown in Fig. 13(c).



**Fig. 13.** Microstructure of processed MIG welded using tool 03(Square pin): (a) FSP regions, (b) flow arm under shoulder, and (c) layers under shoulder (x200).

### 3.3 Mechanical Properties

#### 3.3.1 Hardness

Fig. 14 shows the hardness profiles distribution on cross section for MIG welds and FSP specimens. In MIG welds the hardness decrease at weld zone to 63 HV0.2, a decrease of approximately 15%. This decrease due to increasing the heat of the weld zone, and therefore the cooling rate will be decreased, and, as a result, the grains in the weld zone will be coarser. Therefore, it can cause a decrease in the hardness [22, 23].

The hardness values of FSP specimens processed by cylindrical and square pin tools increases at processed zone compared with base metal and MIG welds. These increased due to the formation of very fine grains in the processed zone caused by severe plastic deformation during friction stirring. While, The hardness of specimens processed by pinless tool was measured on the cross section at 0.25 mm from the weld surface, and on the weld top surface before and after FSP. In both cases was observed, the hardness increase at processed zone under shoulder compared with base metal and MIG welds, these increased due to the tool is better than the others tools where, the surface of shoulder has effective for improve grains and eliminate MIG weld defects that previously showed in microstructure. Fig. 15 shows the hardness profiles distribution on the weld top surface before and after FSP by pinless tool.



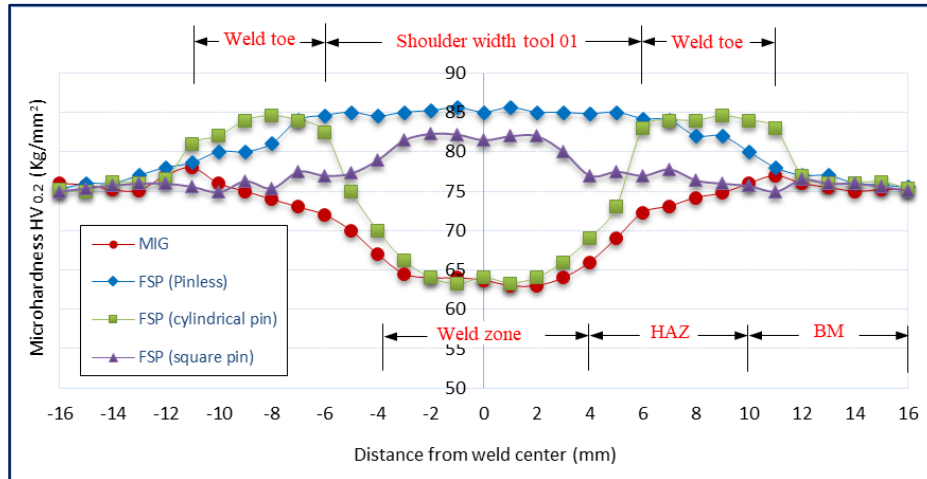


Fig. 14 Microhardness profiles on cross section for MIG welds and FSP specimens.

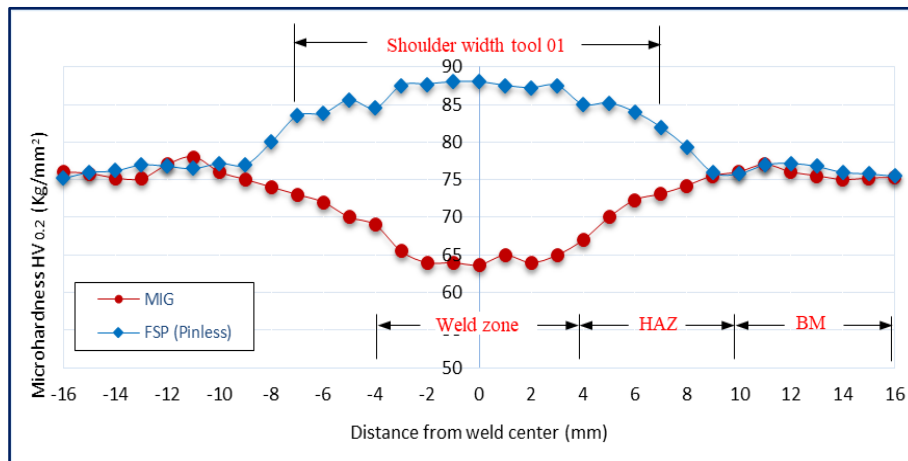


Fig. 15 Microhardness profiles on the weld top surface before and after FSP by pinless tool.

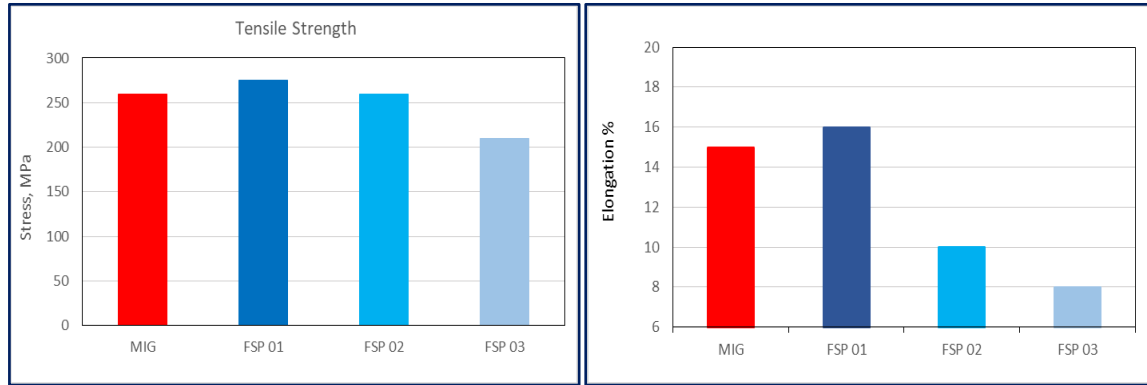
### 3.3.2 Tensile Properties

Tensile tests were performed in this research to study the effects of FSP tool geometry on the tensile strength and elongation of MIG welded. Table 6 represented the tensile test results for different specimens (base metal, MIG welds, and FSP of MIG welds). According to this table, the measured tensile strength and elongation for the base metal were 285 MPa and 20 %, respectively. The tensile strength, and elongation of MIG welds are lower than base metal and the fracture for these specimens occurred in the weld zone.

From Table 6 the results of the tensile test of specimens processed by pinless tool shows increase in tensile properties when compared with MIG welds, these increased are supported by the microstructure results that previously. Where, the grains in the weld metal will be coarser. While, the stirred zone by pinless tool, contained smaller grains and finer precipitates than those found in in MIG welds as a result of dynamic recrystallization during FSP. Fig. 16 shows the comparison of tensile strength and elongation of MIG welds vs. all FSPs. As shown in Fig. 16 (a), joints processed by pinless tool have higher tensile strength compared with those processed by other tools. The tensile strength in FSP 01 was 4.5% lower than base metal, while, strength decrease was about 9% in MIG welds. Also, the joints processed in FSP 02 and FSP 03 shows decrease tensile strength and elongation. This reduction in the strength in both FSPed and MIG joints is common, that is because, as mentioned before, AA5083-H111 is a non-heat treatable alloy. FSP 01 of MIG weld surfaces by pinless is effective process for improve grain structure and increase in both hardness and strength.

**Table 6.** The tensile properties results for different specimens.

Type	Yield strength YS (MPa)	Ultimate tensile strength UTS (MPa)	Elongation %	Fracture Zone
BM (5083)	125	285	20	--
MIG	115	260	15	WZ
FSP 01 (Pinless)	123	275	16	Nugget
FSP 02 (cylindrical)	111	260	10	Toe RS
FSP 03 (square pin)	110	200	8	Outside shoulder



(a)

**Fig. 16** Comparison of tensile properties of MIG welds vs. all FSPs: (a) tensile strength, (b) percentage of elongation.

#### IV. Conclusions

In this research, the effect of FSP tool geometry (pinless, cylindrical pin, and square pin) on microstructure and mechanical properties of MIG welded AA5083-H111 was investigated. The following points can be concluded:

1. The microstructure of MIG welded contains dendritic structure, and solidification porosity defects. In addition, the weld toe contains lack of wetting-defects.
2. Friction stir processing is an efficient method for improve the microstructure and eliminate previous MIG welds defects such as porosity, and lack of wetting.
3. Friction stir processing by pinless tool improved the tensile strength when compared with MIG welds and others tool geometries (cylindrical pin tool, square pin).
4. The hardness increased in the processed zone when compared with base metal and MIG welds, where FSP specimens has a higher hardness value of 88 HV, while the hardness of MIG welds reaches in the melted zone 63 HV.

#### References

- [1]. E. L. Rooy, Introduction to Aluminum and Aluminum Alloys, *Properties and Selection Nonferrous Alloys and Special-Purpose Materials* (ASM International Handbook Committee, USA, 1992) Vol. 2.
- [2]. D. Klobcar, L. Kosec, A. Pietras, and A. Smolej, Friction Stir Welding of Aluminium alloy 5083, *Materiali in tehnologije / Materials and technology*, Vol. 46, 2012, PP. 483-488.
- [3]. K. J. Colligan, Friction Stir Welding for Ship Construction, Concurrent Technologies Corporation (CTC), www.nmc.ctc.com, .2007, PP. 1-6.
- [4]. J. Silva, J. M. Costa, A. Loureiro, and J.M. Ferreira, Fatigue behaviour of AA6082-T6 MIG welded butt joints improved by friction stir processing, *Materials and Design*, Vol. 51, 2013, PP. 315- 322.
- [5]. M. S. Weglowski, Friction stir processing-State of the art, *Archives of Civil and Mechanical Engineering*, Vol. 18, 2018, PP. 114-129.
- [6]. A. Chaudhary, A. K. Dev, A. Goel, R. Butola, and M. S. Ranganath, The Mechanical Properties of Different alloys in friction stir processing: A Review, *Materials Today: Proceedings* 5, 2018, PP. 5553-5562.
- [7]. M. K. Mishra, A. G. Rao, I. Balasundar, B. P. Kashyap, and N. Prabhu, On the microstructure evolution in friction stir processed 2507 super duplex stainless steel and its effect on tensile behaviour at ambient and elevated temperatures, *Materials Science & Engineering A*, Vol. 719, 2018, PP. 82- 92.
- [8]. R. V. Vignesh, and R. Padmanaban, Influence of friction stir processing parameters on the wear resistance of aluminium alloy AA5083, *Materials Today: Proceedings*, Vol. 5, 2018, PP. 7437-7446.
- [9]. C. Gunter, M. P. Miles, F. C. Liu, and T.W. Nelson, Solid state crack repair by friction stir processing in 304L stainlesssteel, *Journal of Materials Science & Technology*, Vol. 34, 2018, PP. 140- 147.
- [10]. J.S. Jesus, J. M. Costa, A. Loureiro, and J.M. Ferreira, Fatigue strength improvement of GMAW T-welds in AA 5083 by friction-stir processing, *International Journal of Fatigue*, Vol. 97, 2017, PP. 124-134.
- [11]. J. S. Jesus, A. Loureiro, J. M. Costa, and J. M. Ferreira, Effect of tool geometry on friction stir processing and fatigue strength of MIG T welds on Al alloys, *Journal of Materials Processing Technology*, Vol. 214, 2014, PP. 2450-2460.

- [12]. L. P. Borrego, J. M. Costa, J. S. Jesus, A. Loureiro, and J. M. Ferreira, Fatigue life improvement by friction stir processing of 5083 aluminum alloy MIG butt welds, *Theoretical and Applied Fracture Mechanics*, Vol. 70, 2014, PP. 68-74.
- [13]. C.B. Fuller, and M. W. Mahoney, The Effect of Friction Stir Processing on 5083-H321/5356 Al Arc Welds: Microstructural and Mechanical Analysis, *Metallurgical and materials transactions A*, Vol. 37, 2006.
- [14]. S. A. Eshraghi, *Mechanical Properties of Fine Grain 5083 Aluminum Alloy*, Doctor Thesis, University of California, Irvine, 2005.
- [15]. AWS D1.2/D1.2M, Structural Welding Code-Aluminum, an American National Standard, sixth Edition, 2014.
- [16]. M. A. T. Obregon, *Effect of Process Parameters on Temperature Distribution, Microstructure, and Mechanical Properties of Self-Reacting Friction Stir Welded Aluminum Alloy 6061-T651*, M.Sc.Thesis, the University of Texas at El Paso, 2011.
- [17]. C. J. Sterling, Effects of Friction Stir Processing on the Microstructure and Mechanical Properties of Fusion Welded 304L Stainless Steel, M.Sc. Thesis, Brigham Young University, 2004.
- [18]. ASTM Standard E3-11, Standard Guide for Preparation of Metallographic Specimens, ASTM International, West Conshohocken, PA, 2011.
- [19]. ASTM Standard E407-07, Standard Practice for Microetching Metals and Alloys, ASTM International, West Conshohocken, PA, 2011.
- [20]. ASTM Standard E384-11e1, Standard Test Method for Knoop and Vickers Hardness of Materials, ASTM International, West Conshohocken, PA, 2012.
- [21]. ASTM Standard E8M-4, Standard Test Methods for Tension Testing of Metallic Materials, ASTM International, West Conshohocken, PA, 2004.
- [22]. A. R. Yazdipour, A. Shafiei, H. J. Aval, An investigation of the microstructures and properties of metal inert gas and friction stir welds in aluminum alloy 5083, *Sadhana*, Vol. 36, 2011, PP. 505-514.
- [23]. E. M. ELSayed, A. Y. A. Mohamed, M. M. Z. Ahmed, A. EL-Nikhaily, Effect of friction stir processing on the mechanical properties and microstructure of cast aluminum (Al-Si-Zn-Cu) Alloy, *Engineering research journal*, Vol. 137, 2013, PP. 79-93.

H. H. El-Fahhar "The Effect of Tool Geometry on the Microstructure and Mechanical Properties of Friction Stir Processed MIG-Welded AA5083-H111." *IOSR Journal of Mechanical and Civil Engineering (IOSR-JMCE)*, vol. 15, no. 4, 2018, pp. 45-55